Available online at www.sciencedirect.com

Catalysis Today 107–108 (2005) 388–396

www.elsevier.com/locate/cattod

Theoretical study of dimeric dioxo-μ-oxo and oxo-bis (μ-oxo) of molybdenum complexes used in catalytic oxidations reactions

Beulah Griffe [a,*], Giuseppe Agrifoglio [b], Joaquín L. Brito [a], Fernando Ruette [c]

[a] *Laboratorios de Físico-Química de Superficies, Centro de Química, Instituto Venezolano de Investigaciones Científicas, I.V.I.C., Apartado 21827, Caracas 1020-A, Venezuela*

[b] *Polímeros, Centro de Química, Instituto Venezolano de Investigaciones Científicas, I.V.I.C., Apartado 21827, Caracas, 1020-A, Venezuela*

[c] *Química Computacional, Centro de Química, Instituto Venezolano de Investigaciones Científicas, I.V.I.C., Apartado 21827, Caracas, 1020- A, Venezuela*

Available online 1 September 2005

Abstract

In this work dimeric complexes, dioxo-μ-oxo and oxo-bis (μ-oxo) of molybdenum, were theoretically modeled to try to understand reactivity for hydrocarbon oxidation. The first complex, dioxo (μ-oxo) thiocyanatomolybdenum (VI) bearing a 4,4′-di-ter-butyl-2,2′-bipyridine ligand (complex **1**) in *trans* conformation exhibits a high oxidizing ability, giving as product a dimeric complex oxo-bis (μ-oxo) thiocyanatomolybdenum (V) with the same ligands (complex **2**) in *cis* conformation. Calculations were perfomed by using CATIVIC, a parametric quantum chemistry method for catalytic reactions. Furthermore, new geometries were created, using the CATIVIC graphic interface, starting with complex **1** to transform it to *cis* conformation (complex **3**). Molecular parameters for Mo were estimated from diatomic molecules and molecular properties, such as charges, interatomic distances, bond orders, and diatomic energies of selected bonds, and atoms were calculated for these complexes. In addition, LUMO characteristics were evaluated and discussed. Results suggest the feasibility of complex **1** transformation through a bridge Mo–O bond rotation to form complex **3** that is energetically less stable than complex **1** in 21 kcal/mol. Results of bond strength indicate a high lability of the bipyridine ligand and a high LUMO density of states in *cis* conformation. Preliminary steps of the mechanism for the formation of a highly active site that explains the oxidizing ability of complex **1** is given by considering the rotation through a bridging Mo–O bond to form a *cis* complex **3** and then a Mo–N bond breaking. Vacancy creation could be considered as a previous step to the formation of active sites for catalytic oxidation.

© 2005 Elsevier B.V. All rights reserved.

Keywords: Theoretical modeling; Molybdenum oxide complex; CATIVIC; Catalytic oxidation

1. Introduction

In the important field of transition-oxo chemistry, molybdenum is of special interest, since it is found in many catalytic systems going from molybdenum enzymes to heterogeneous reactions on metal oxides [1–3]. Molybdenum–oxo complexes have been studied in oxygen atom transfer (OAT) processes, for instance the oxo transferase enzymes like nitrate reductase in which the active sites consist of a *cis* molybdenum dioxo moiety.

Arzoumanian et al. have studied various molybdenum complexes capable of transferring oxygen atom to different substrates [4–6]. Recently they investigated more in detail a molybdenum (VI) dioxo compound **1** that exhibits exceptional oxo-transfer capabilities [7]. It is a μ-oxo dimer bearing thiocyanato groups and a bulky 4,4′-di-ter-butyl-2,2′-bipyridine ligand. All thiocyanato molybdenum dioxo compounds have been shown to catalyze the oxidation of phosphanes and alcohols in presence of oxygen atom donors

---

* Corresponding author.
E-mail address: bgriffe@ivic.ve (B. Griffe).

0920-5861/$ – see front matter © 2005 Elsevier B.V. All rights reserved.
doi:10.1016/j.cattod.2005.07.162

such as DMSO, to give the corresponding phosphane oxide and ketone or aldehyde [5,6].

In the absence of oxidixing agent, **1** reacts readily either with excess arylphosphine, alkylphosphine or an alcohol such as 2-ethoxyethanol to give upon work a crystalline solid **2**.

An important breakthrough in the use of organomolybdenum oxide in oxidation catalysis, was the isolation **2** and its X-ray characterization from two different reactions, starting from complex **1**

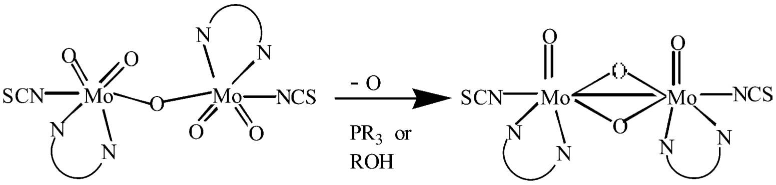

Complex (**1**) Complex (**2**) (1)

where  is the 4,4′-di-ter-butyl-2,2′-bipyridine ligand.

Complex **1** shows an unusual case of a μ-oxo conformational equilibrium. In its crystal structure, the cell unit was found to contain three molecules of **1**, one with a Mo–O–Mo angle of 180° (*meso*) and other two with an angle of 155.7° (d,l pair). The NMR-spectroscopy [7] shows also the presence of both, *meso* and d,l conformers.

The chemical transformation of **1** in **2** was followed by UV and NMR spectroscopies. These techniques show clearly a very complex evolution with the probable presence of, either a short lived intermediate(s) preceding the formation of **2**, or an *anti* isomer of **2**, which rearranges to the final isomer *syn* [8]. Such intermediate could be of utmost importance in catalytic oxidation processes.

Pellegatti et al. [9] recently published a paper about ab initio theoretical calculations of complex **1**. The authors fragmentize the molecule and concluded that the *meso* form and d,l form have practically the same energy. They use the fragmentation to compare with the complete molecule and demonstrate that *t*-butyl groups and even pyridyl rings play a minor role in determining the electronic structure.

The objective of this work is to model these complexes using a parametric code CATIVIC [10,11] in order to propose an explanation of intermediates in the formation of complex **2**. For example, to explain why the reactive substrate being a *trans* (complex **1**), the final product after reduction has a *cis* conformation (complex **2**), independently of the type of reactant (ROH or PR_3). The theoretical method used here was employed because it allows to obtain qualitative information for large systems, in this case, molecules of 100 and 101 atoms. Furthermore, geometries were generated of opposite configurations for complexes **1** and **2** with its graphic interface. Bonding properties were calculated to understand the role of terminal and bridging oxygens, other ligands, and Mo interactions in oxidation reactions.

This paper is organized in the following way. Details of the method, parameterization, and evaluated properties are described in Section 2. In Section 3, the description of modeling is presented. Properties of complexes **1**, **2** and rotational conformers, LUMO characteristics, and formation of active site are presented in Section 4. Final remarks are described in Section 5.

2. Computational and theoretical details

A quantum chemistry parametric method for catalytic reactions denominated CATIVIC [10–16] was employed. This method is based on simulation techniques, using parametric functionals to mimic the total energy functional [17–19]. Details of atomic and molecular parameterization processes used in this method are presented elsewhere [10,11].

Atomic parameters for H, O, C, N, S molecular parameters for H–H, H–O, H–C, H–N, H–S, C–O, C–N, C–S, C–C, N–O, N–S, N–N and S–S are those used in MINDO/SR method [20]. Nevertheless, values for Mo were calculated using a different methodology as shown in Ref. [11]. Molecular parameters α and β were obtained by adjusting them to obtain dissociation energy (−56.1, −115.5, −117.6, 116.0, −81.4, −97.1 kcal/mol) and equilibrium bond distance (1.68, 1.676, 1.636, 1.70, 2.212, 1.938 Å) of the experimental data for Mo–H [21], Mo–C [22], Mo–N [23], Mo–O [24], and Mo–Mo [25] diatomic molecules and of Mo–S bond in MoS_2 [26], respectively. The optimal values of parameters (beta (β) for the electronic and alpha (α) for the core–core interaction functionals) are reported in Table 1.

Theoretical tools used for evaluating the bond strengths: diatomic energies (DE), and bond orders (BO) (Wiberg

Table 1
Molecular parameters alpha and beta for Mo–X (X=H, C, N, O, S, Mo)

Parameters pair of atoms	β	α
Mo–Mo	0.477511	1.17590232
Mo–H	0.345575	1.72163554
Mo–C	0.501717	1.67371964
Mo–N	0.531452	1.68918634
Mo–O	0.942650	2.54236675
Mo–S	0.458245	2.14290654

index) are reported elsewhere [27,28]. DE comes from the total energy partition that can be easily performed in parametric methods. Others properties were evaluated: equilibrium bond distances (EBD), atomic charges, and atomic orbital population.

Some applications of CATIVIC have been published [13–16]. Thus, in [13] calculations of several beryllium complexes were carried out to compare ab initio (density functional theory, MP2) and parametric PM3, CATIVIC methods. Results show that CATIVIC gives geometries that are closer to the ab initio than PM3 method. In [14], the formation of amino acids, on the surface of polycyclic aromatic hydrocarbon flake (coronene) is studied with CATIVIC, and it is reported a chemisorption energy of +2.27 eV, which compares satisfactorily with +2.58 eV computed with Gaussian 98 (B3LYP/3-21G). Recently in [16], the application of this code to catalytic systems is illustrated with several examples, which include the study of size effect on zeolite adsorption site, the location of Al and Fe adsorption sites, and formation of Al extra-red in zeolites.

It is convenient to mention that CATIVIC is based on MINDO/SR method [29]. This last method has been successfully applied to catalytic reactions [30,31]. As stated above, theoretical foundations of these methods are based on simulation techniques referenced to a set of molecules. In our case, we use diatomic molecules, because modeling in physics always starts firstly with the simplest systems, as it was applied in previous works [29–31]. However, more precise methods may be fashioned to adjust parameters from the matching functionals. Thus, a set of polyatomic molecules (not only diatomic) can be used in order to find the best functionals and the corresponding parameters. Some of these developments are in progress [32,33].

3. Modeling

Models of real complexes were obtained from the coordinate crystallographic structures [34] of dioxo (μ-oxo) thiocyanatomolybdenum (VI) bearing 4,4′-di-ter-butyl-2,2′-bipyridine ligands (complex **1**), in *trans* conformation, and oxo-bis (μ-oxo) thiocyanatomolybdenum (V) 4,4′-di-ter-butyl-2,2′-bipyridine (complex **2**) in *cis* conformation. These complexes are shown in Figs. 1 and 2.

Geometry of complex **3** was generated by using the graphic interface of CATIVIC and can be seen in Fig. 3. Complex **3** was obtained from complex **1**, in which part of the molecule is maintained fixed (a Mo atom with all

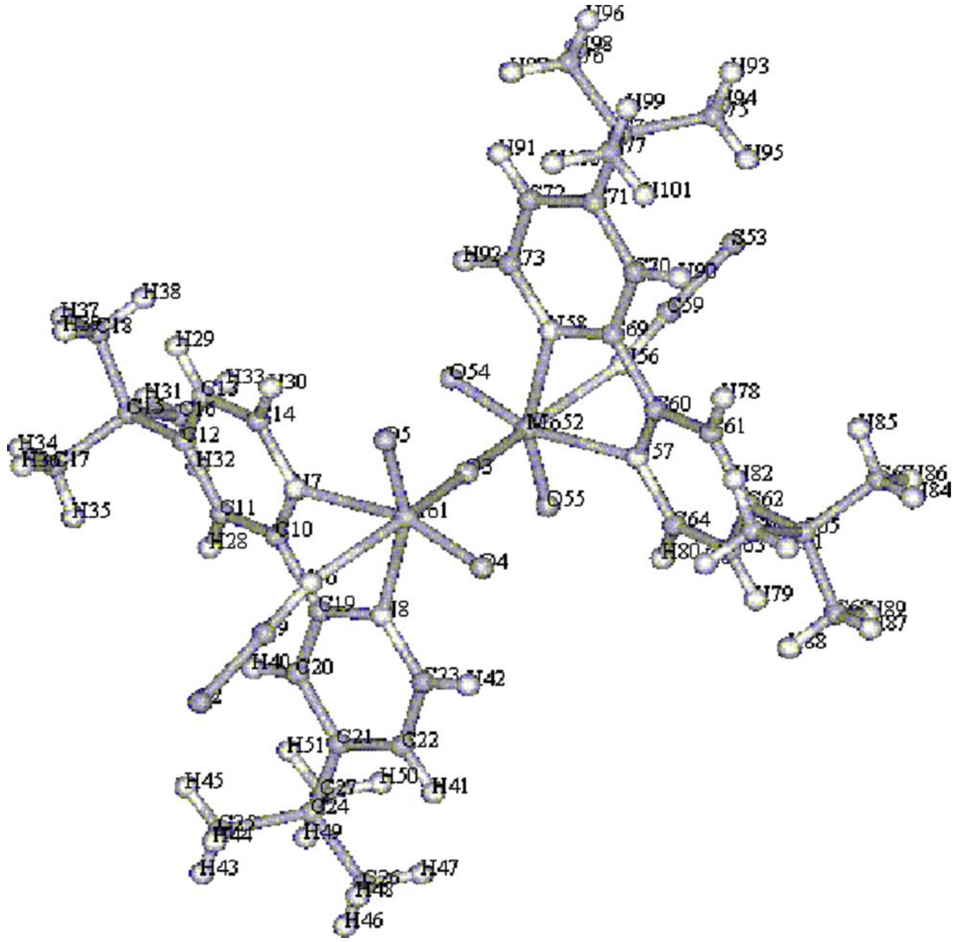

Fig. 1. Structure of thiocyanatomolybdenum (VI) dioxo (μ-oxo) complex dimer bearing a 4,4′-di-ter-butyl-2,2′-bipyridine ligands d,l (complex **1**).

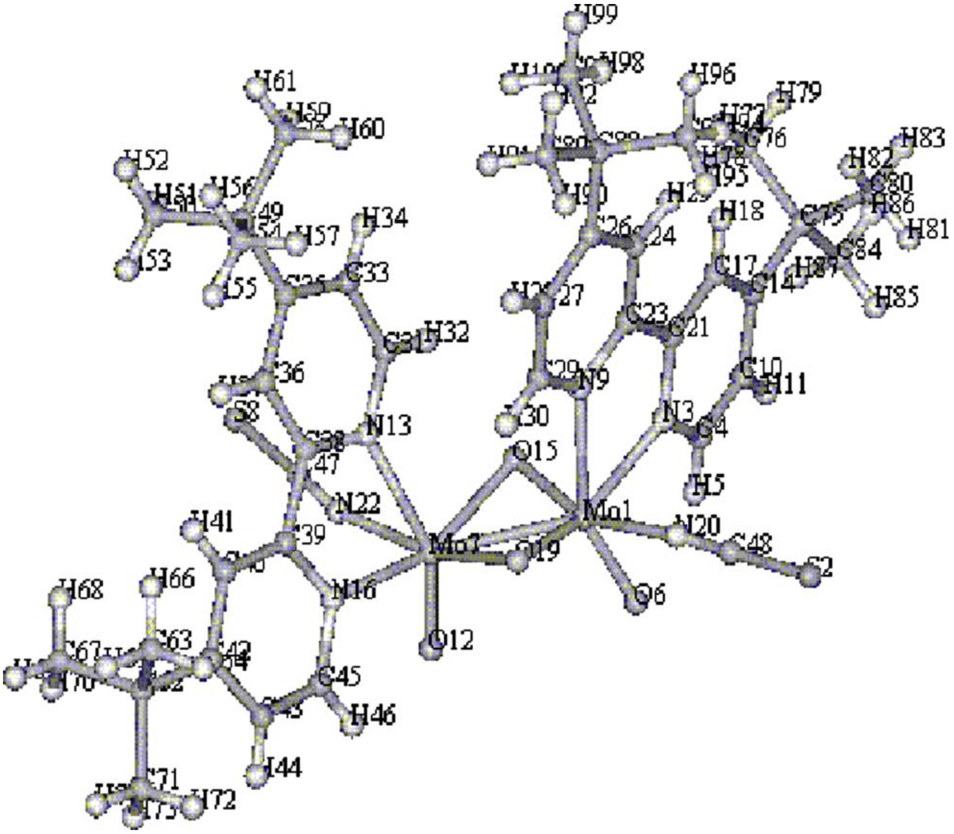

Fig. 2. Structure of thiocyanatomolybdenum (V) oxo-bis-(μ-oxo) complex dimer bearing a 4,4′-di-ter-butyl-2,2′-bipyridine ligands (complex **2**).

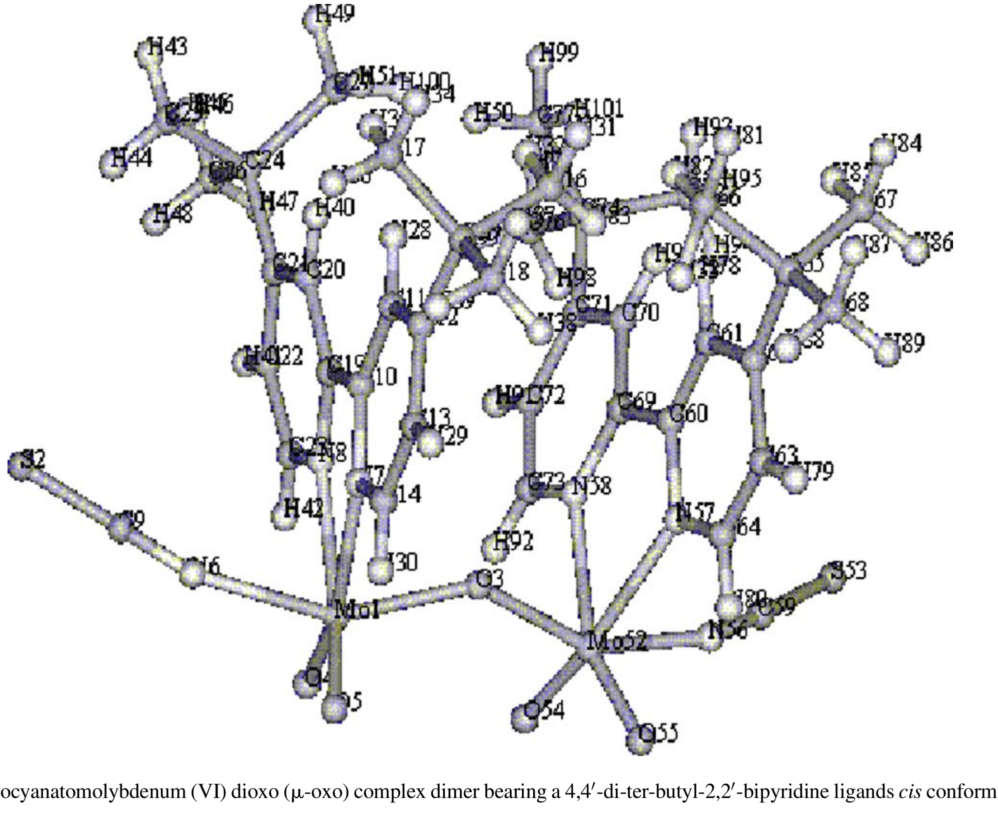

Fig. 3. Structure of thiocyanatomolybdenum (VI) dioxo (μ-oxo) complex dimer bearing a 4,4′-di-ter-butyl-2,2′-bipyridine ligands *cis* conformation (complex **3**).

ligands), and the other part of the molecule is rotated through a Mo–O bond to simulate a *cis* conformation. This interface allows to create by hand different starting point for optimization of conformer generated in the calculation of rotational energy curve.

4. Results and discussion

4.1. Bond properties of complex *1*

Results of charge, orbital population, BO and DE, for a selected set of atoms and bonds of complex **1** are shown in Table 2. Calculation was carried out with the experimental geometry. Numeration of atoms is shown in Fig. 1. Charge distribution indicates that Mo atoms have spd hybridization with an important electronic transference to the p orbitals. A depletion of Mo electronic s- and d-densities is observed when comparing the free atomic population ($s^1p^0d^5$) with the corresponding one in the complex ($s^{0.54}p^{1.11}d^{3.93}$). In addition, an electronic charge transfer to the ligands of (0.42 a.u.) is obtained. S atoms are the most negatively charged (−0.55 a.u.) followed by N (−0.24 a.u.) of thiocyanato ligands, O terminals (−0.17 a.u.), O bridge (−0.13 a.u.), and N of bipyridine ligands (−0.07 a.u.).

Table 2
Summary of atomic and molecular properties of thiocyanatomolybdenum (VI) dioxo (μ-oxo) complex dimer bearing a 4,4′-di-ter-butyl-2,2′-bipyridine ligands (complex **1** shown in Fig. 1)

Atom	Charge	Orbital population		
		s	p	d
Mo1	0.42	0.54	1.11	3.93
N6	−0.24	1.50	3.75	–
S2	−0.55	1.89	4.66	–
O3	−0.13	1.46	4.67	–
Mo52	0.42	0.54	1.11	3.93
N56	−0.24	1.50	3.75	–
S53	−0.55	1.89	4.66	–
O4	−0.16	1.56	4.61	–
O5	−0.17	1.56	4.61	–
N7	−0.07	1.52	3.55	–
N8	−0.07	1.52	3.55	
C9	0.35	1.34	2.31	–
N49	−0.25	1.49	3.75	–
O54	−0.16	1.56	4.61	–
O55	0.17	1.56	4.61	–
N57	−0.07	1.52	3.55	–
N58	−0.07	1.52	3.55	–
C59	0.35	1.34	2.31	–

Pair	EBD (Å)	DE (a.u.)	Wiberg index
O3–Mo1	1.72	−1.00	2.42
O4–Mo1	1.72	−1.00	2.41
Mo1–O5	2.06	−0.44	1.11
Mo1–N6	2.11	−0.27	0.68
N7–Mo1	2.32	−0.12	0.29
Mo52–O3	1.88	−0.45	1.21
Mo52–O54	1.69	−0.97	2.33
Mo52–O55	1.70	−0.96	2.32
Mo52–N56	2.11	−0.27	0.68
Mo52–N57	2.32	−0.12	0.29
Mo52–N58	2.31	−0.13	0.30
Mo52–Mo1	3.75	−0.06	0.04

Bond strengths show two types of Mo–O interactions: a first one that has double-bond nature (terminal O) and another that is single-bond in character (bridging O). They correspond to EBDs of 1.69 and 1.88 Å that give BOs of 2.42 and 1.11, and DEs of −0.45 and −0.97 a.u., respectively. In a similar way, Mo–N bonds with EBDs of 2.11 and 2.32 Å are associated to weak BOs of about 0.69 and 0.29 and DEs of −0.27 and −0.13 a.u. Notice that the bipyridine ligands have two anchor sites. These small values of BO and DE for Mo–N interaction, specially the bipyridine ligand, indicate very labile groups. Mo–Mo is very weak with a DE of −0.06 a.u. and a bond index of 0.04 due to the long Mo–Mo distance (3.75 Å).

4.2. Bond properties of complex *2*

Complex **2** is the resultant product of complex **1** after hydrocarbon oxidation as shown in scheme (1). The atomic and bond properties of this complex are summarized in Table 3, for a selected set of atoms and bonds using as input

Table 3
Summary of atomic and molecular properties of thiocyanatomolybdenum (V) oxo-bis-(μ-oxo) complex dimer bearing a 4,4′-di-ter-butyl-2,2′-bipyridine ligands (complex **2** shown in Fig. 2)

Atom	Charge	Orbital population		
		s	p	d
Mo1	0.40	0.45	0.97	4.18
S2	−0.61	1.89	4.71	–
Mo7	0.36	0.45	0.96	4.23
S8	−0.62	1.90	4.72	–
N20	−0.26	1.49	3.76	–
N22	−0.22	1.48	3.74	–
N3	−0.01	1.49	3.52	–
O6	−0.11	1.56	4.55	–
N9	−0.07	1.53	3.54	–
O15	−0.19	1.54	4.65	–
O19	−0.20	1.54	4.66	–
C48	0.33	1.32	2.35	–
O12	−0.11	1.56	4.55	–
N13	−0.06	1.53	3.53	–
N16	0.01	1.50	3.51	–
C47	0.31	1.32	2.37	–

Pair	EBD (Å)	DE (a.u.)	Wiberg index
Mo1–N3	2.22	−0.76	0.43
Mo1–O6	1.68	−1.02	2.46
Mo1–Mo7	2.55	−0.18	0.50
Mo1–N9	2.33	−0.11	0.25
Mo1–O15	1.93	−0.39	1.14
Mo1–O19	1.91	−0.44	1.24
Mo1–N20	2.20	−0.24	0.58
Mo7–O12	1.68	−1.02	2.47
Mo7–N13	2.31	−0.11	0.26
Mo7–O15	2.93	−0.41	1.18
Mo7–N16	2.23	−0.17	0.42
Mo7–O19	1.94	−0.36	1.08
Mo7–N22	2.17	−0.24	0.60

the experimental geometry. Atom numbers are shown in Fig. 2. Positive charge on Mo atoms (0.38 a.u.) is smaller than in complex **1** (0.42) because of reduction caused by the O transfer to the hydrocarbon. There is also an electronic rearrangement in complex **2** ($s^{0.45}p^{0.97}d^{4.18}$) because d population increases and s and p ones decrease respect to complex **1** ($s^{0.54}p^{1.11}d^{3.93}$).

The average value of DE (−1.02 a.u.) and BO (2.46) of terminal Mo–O bonds in complex **2** indicates stronger bonds than in complex **1** (DE = −0.97 a.u. and BO = 2.32). On the other hand, bridge Mo–O average bonds are weaker in the former (DE = −0.40 a.u. and BO = 1.16) than in the latter (DE = −0.45 a.u. and BO = 1.21). Mo–N bond in thiocyanato group has a DE = −0.24 a.u. and a BO = 0.60 that are smaller than the corresponding of complex **1** (DE = −0.27 a.u. and a BO = 0.68). In similar way, a decrease of Mo–N bipyridine bonds is observed with respect to complex **1** because now the system is more rigid due to the formation of two O bridge ligands. The effect of this bond decreasing is also compensated by the formation of a Mo–Mo bond (DE = −0.18 a.u. and BO = 0.50).

4.3. Rotational conformers

Because the final product has a *cis* conformation, one way to visualize the mechanism of transformation to *trans* is by assuming that the complex **1** may rotate through one of the Mo–O bridge bonds before it reacts. Calculations were carried out for different dihedral angles between O–Mo–O and Mo–O–N planes. In this case, optimization of all atoms was considered, in order to make comparison between complex **1** and complex **3** shown in Fig. 3. Results of optimized complex **3**, see Table 4, with respect to experimental values show an enlargement of all bond distances: Mo–O terminal from 1.69 to 1.72 Å; 1.88 to 2.06 Å in Mo–O bridge; Mo–N of thiocyanato and bypiridine ligands from 2.11 and 2.32 to 2.24 and 2.55 Å, respectively.

A graphic illustration of total binding energy change from complex **1** to **3** versus dihedral angle is shown in Fig. 4. The periodicity was of 30° of the dihedral angle of the second molybdenum. The variation from complex **1** to **3**, see Figs. 1 and 3, were performed in both ways using CATIVIC's graphic interface and with the program fixing part of the molecule, changing the other part to internal coordinates by varing the dihedral angle to turn the molecule step by step. In addition, the calculation was carried in two directions: one starting with optimized complex **1** and other beginning with complex **3** in both cases the calculation through the energy curve starts with the Fock matrix of a previous dihedral angle. As can be seen in Fig. 4, there is a difference of 21 kcal/mol from complex **1** to the complex **3**. This difference could suggest the possibility of complex **1** going to **3**, as an intermediate in the oxygen transferring. The energetic barrier of about 28 kcal/mol is mainly due to repulsive interactions between the two bulky bipyridine groups. This fact could be compensated by a major accessibility to the reaction site, due to the fact that the reactant (olefine or phosphine) could reach more easily the reactive site. The oxidation would take place with the loss of an oxygen atom. The rearrangement to arrive at complex **2** with two bridged Mo–O–Mo and two terminal Mo=O could be explained by results reported by Crabtree et al. [35] in which $M–(\mu\text{-}O)_2–M$ is in equilibrium with M–O–M=O.

Table 4
Summary of atomic and molecular properties of optimized complex **3**, shown in Fig. 3

Atom	Charge	Orbital population		
		s	p	d
Mo1	0.49	0.55	1.08	3.89
N6	−0.25	1.49	3.75	–
S2	−0.51	1.89	2.62	–
O3	−0.31	1.54	4.76	–
Mo52	0.49	0.55	1.08	3.89
N56	−0.25	1.49	3.76	–
S53	−0.51	1.89	4.61	–
O4	−0.11	1.57	4.54	–
O5	−0.12	1.57	4.54	–
N7	−0.10	1.53	3.57	–
N8	−0.10	1.53	3.57	–
C9	0.37	1.35	2.28	–
O54	−0.11	1.57	4.54	–
O55	−0.12	1.57	4.54	–
N57	−0.10	1.53	3.57	–
N58	−0.10	1.53	3.57	–
C59	0.37	1.35	2.28	–

Pair	EBD (Å)	DE (a.u.)	Wiberg Index
Mo1–O3	2.06	−0.44	1.11
O4–Mo1	1.72	−1.00	2.42
O5–Mo1	1.72	−1.00	2.41
Mo1–N6	2.55	−0.10	0.20
Mo1–N7	2.56	−0.10	0.20
Mo1–N8	2.24	−0.29	0.72
O3–Mo52	2.06	−0.44	1.11
Mo52–O54	1.72	−1.00	2.42
Mo52–O55	1.72	−1.00	2.41
Mo52–N56	2.24	−0.29	0.72
Mo52–N57	2.55	−0.10	0.20
Mo52–N58	2.56	−0.10	0.20
Mo52–Mo1	4.13	−0.04	0.03

4.4. LUMO properties

The complex **1** undergoes a reduction after oxidizing hydrocarbons or phosphines, therefore the nature of frontier orbital LUMO can give information about reactivity for the acceptance of electrons. LUMO energies for complexes **1** and **3** are presented in Table 5 in order to compare reactivity. Results indicate that the complex **3** has a higher number of LUMO's (a higher density of states) than complex **1**. Notice that all orbitals in complex **3** have components in Mo and O atoms. It could imply major capability of receiving electrons (to be reduced) and thus to oxidize another molecule. Therefore, rotation of complex **1** thorough Mo–O

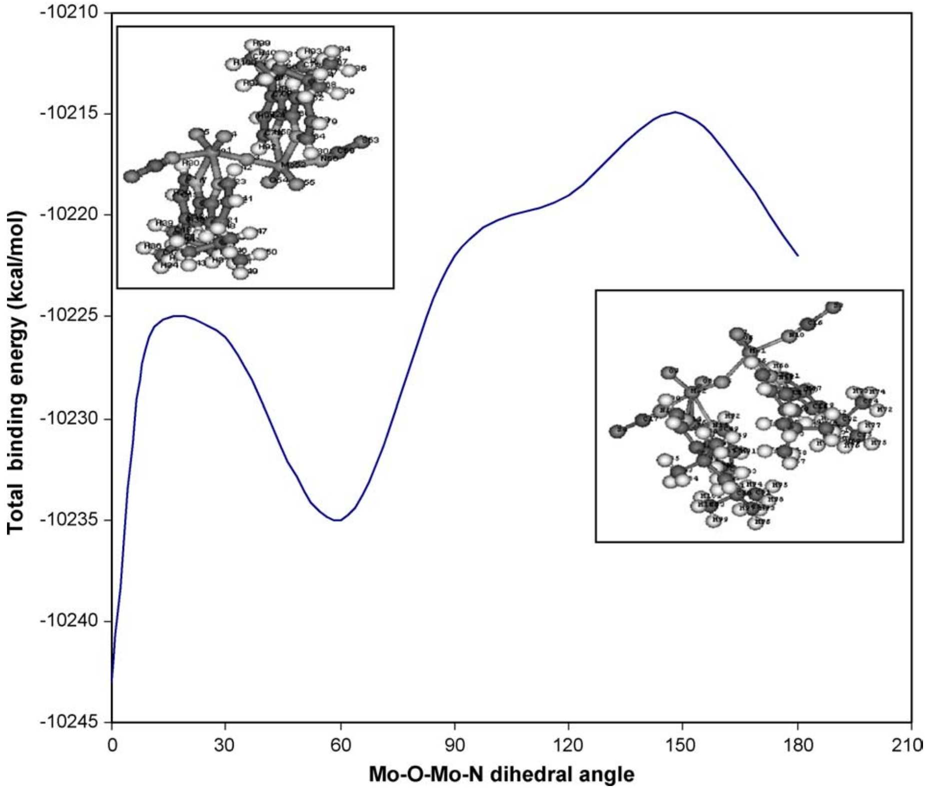

Fig. 4. Changes of total binding energy of complex **1**–**3** transformation vs. dihedral angle.

bond to produce complex **3** could be very important to explain the high reactivity of these oxo compounds. Following these preliminary results, it could be suggested that complex **1** could evolve to complex **3**, then transfers an oxygen to the olefin, then remaining oxygen atoms rearrange to form the bridged structure, as suggested by Crabtree [35] and the structure of the product would be *cis*, as shown in complex **2**.

4.5. Proposed mechamism steps

Results of Section 4.3 indicate that formation of a rotamer with a *cis* conformation may occur, see scheme (2). Here, L_1 and L_2 are thiocyanato and 4,4′-di-ter-butyl-2,2′-bipyridine ligands, respectively. Values of total binding energy are displayed below each compound, in parentheses. There, a change of 21 kcal/mol was obtained for a rotation through a Mo–O bridge bond.

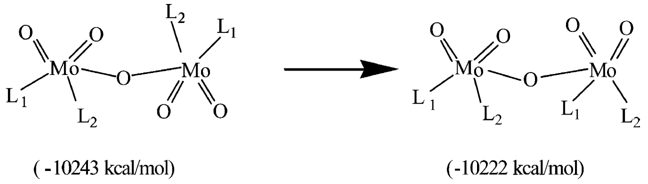

(2)

On the other hand, the high lability of the bipyridine ligands (L_2), as mentioned above, suggests a possible mechanism for the formation of an active site may go through a step in which L_2 ligand is lost, as shown in scheme (3). In fact, a small amount of energy (23 kcal/mol) is calculated to break the Mo–L_2 bond.

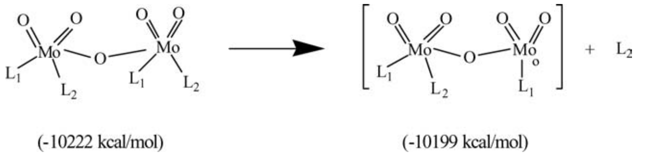

(3)

Notice that in this process we consider the scission of two Mo–N bonds in the bipyridine ligand. However, there is also the possibility of only one single bond being broken. This option will keep the L_2 ligand close to the vacancy site.

Notice that the formation of vacancy in one of the Mo atoms (see Mo_o in scheme (3)) may generate an asymmetric charge distribution in metallic centers, as well as terminal

Table 5
Energetic characteristics and atomic orbital composition of LUMOs for **1** and **3** complexes

Complex **1**		Complex **3**	
Composition	Energy	Composition	Energy
(Mo, S, O, N)	−0.01367	(Mo, N, C, S, O)	−0.01058
(C–N)	−0.00654	(Mo, C, S, O, N)	−0.00953
–	–	(Mo, O)	−0.001044

Energy units are in a.u.

oxygen atoms. This could be the previous step for active species generation. More calculations have to be carried out in order to describe the formation of the active site, the oxidation pathway and the formation of complex **2**. Problems of convergence electronic occur because two different oxidation states (Mo (V) and Mo (VI)) arise with the formation of another bridge bond that will lead to the complex **2**.

5. Conclusions and comments

(1) The method CATIVIC parameterized for systems with Mo atoms was applied in the modeling of dioxo (μ-oxo) thiocyanatomolybdenum (VI) 4,4′-di-ter-butyl-2,2′-bipyridine. Qualitative results for geometry optimization (about 10% of experimental data) were obtained. Nevertheless, the advantage of this method is that it can be employed on large molecules (about 100 atoms) with a considerably reduced calculating time.

(2) Calculations for complexes **1** and **2** confirm the existence of single (bridge) and double (terminal) bonds. The Mo atom has a spd hybridization with an important contribution of p orbitals. In the case of complex **2** stabilization is caused by stronger M=O bonds and the formation of a bonding Mo–Mo interaction. This last feature is in concordance with experimental X-ray structure.

(3) Bipyridine ligands show a weak Mo–N bond, indicating a high lability of these ligands that is corroborated by the small energy difference (23 kcal/mol) between the system with and without a bipyridene ligand.

(4) Different conformations were built with CATIVIC graphic interface and calculations for the total binding energy versus the dihedral Mo–O–Mo–N angle. Results indicate that there is an energy difference of 21 kcal/mol between complex **1** and complex **3** (the *cis* conformer of **1**). The energy barrier for this rotation is about 28 kcal/mol.

(5) Results of orbital properties indicate that complex **3** has a major LUMO density of states than complex **1** at Mo and O atoms. This fact suggests that complex **3** should be more reactive for accepting electrons and reducing the Mo site. Therefore, it is expected that a *cis* species of complex **1** would a convenient intermediate in the mechanism of hydrocarbon oxidation.

(6) Preliminary steps to the formation of the active site by transforming complex **1** into complex **3** are proposed. This is based on rotation through a bridge Mo–O bond in **1** to form **3** and the lability of bipyridine ligands. Results also support the fact that *cis* complex **3** is more reactive than the *trans* **1**, because of a higher LUMO density of states in the former. Thus, creation of a vacancy will be a previous step to the formation of an intermediate that will lead to a new bridge Mo–O–Mo bond, as in complex **2**. More work has to be done to understand the reaction pathway, the formation of complex **2** and active sites, as well as for electron donor systems (phosphines) and for electron acceptors ones (alcohols).

Acknowledgment

This research has been partially sponsored by FONACIT, Venezuela, under contract G-9700667.

References

[1] E.I. Stiefel, in: E.I. Stiefel, D. Coucouvanis, W.E. Newton (Eds.), Molybdenum Enzymes Cofactors and Model Systems, American Chemical Society, Washington, DC, 1993, p. 1.

[2] E.I. Stiefel, J. Chem. Soc., Dalton Trans. (1997) 3915.

[3] J.D. Burrington, C.T. Kartisek, R.K. Grasselli, J. Catal. 87 (1984) 363.

[4] H. Arzoumanian, R. López, G. Agrifoglio, Inorg. Chem. 33 (1994) 3177.

[5] H. Arzoumanian, G. Agrifoglio, H. Krentzien, M. Capparelli, J. Chem. Soc. Chem. Commun. (1995) 655.

[6] H. Arzoumanian, L. Maurino, G. Agrifoglio, J. Mol. Catal. A: Chem. 117 (1997) 471.

[7] H. Arzoumanian, R. Bakhtchadjian, G. Agrifoglio, H. Krentzien, J.C. Daran, Eur. J. Inorg. Chem. (1999) 2225.

[8] G. Agrifoglio, Unpublished results.

[9] A. Pellegatti, H. Arzoumanian, B. Blaive, Chem. Eur. J. 9 (2003) 5655.

[10] F. Ruette, M. Sanchez, G. Martorell, C. Gonzalez, R. Añez, A. Sierraalta, L. Rincón, C. Mendoza, Int. J. Quantum Chem. 96 (2004) 321.

[11] F. Ruette, M. Sánchez, C. Mendoza, A. Sierraalta, G. Martorell, C. González, Int. J. Quantum Chem. 96 (2004) 303.

[12] F. Ruette, C. González, Chem. Phys. Lett. 359 (2002) 428.

[13] R. Martínez, F. Brito, M.L. Araujo, F. Ruette, A. Sierraalta, Int. J. Quantum Chem. 97 (2004) 854.

[14] C. Mendoza, F. Ruette, G. Martorell, L.S. Rodrígues, Astron. Astrophys. 601 (2004) L59.

[15] I. Machín, J.C. de Jesús, G. Rívas, I. Higuerey, J. Córdova, P. Pereira, F. Ruette, J. Mol. Catal. 227 (2005) 223.

[16] F. Ruette, M. Sánchez, A. Sierraalta, C. Mendoza, R. Añez, L.S. Rodrígues, O. Lisboa, J. Daza, P. Manrique, Z. Perdomo, M. Rosa-Brussin, J. Mol. Catal. A 228 (2005) 211.

[17] M. Romero, M. Sánchez, A. Sierraalta, L. Rincón, F. Ruette, J. Chem. Inform. Comp. Sci. 39 (1999) 543.

[18] F. Ruette, C. González, A. Octavio, J. Mol. Struct. Theochem 537 (2001) 17.

[19] F. Ruette, S.A.M. Marcantognini, V.V. Karasiev, J. Mol. Struct. Theochem 636 (2003) 15.

[20] G. Blyholder, J. Head, F. Ruette, Theor. Chim. Acta 60 (1982) 429.

[21] M-A. Tolbert, J.L. Beauchamp, J. Phys. Chem. 90 (1986) 5015.

[22] D.J. Brugh, T.J. Ronningen, M.D. Morse, J. Chem. Phys. 109 (1998) 7851.

[23] I. Shim, K.A. Gingerich, Theochem 460 (1999) 123.

[24] Y.M. Hamrick, S. Taylor, M.D. Morse, J. Mol. Spectrosc. 146 (1991) 274.

[25] Handbook of Chemistry and Physics, 76th Ed., CRC Press, NY, 1996, pp. 9–55.

[26] H. Topsoe, B.S. Clausen, N.Y. Topsoe, J.K. Norskov, C.V. Ovesen, C.J.H. Jacobsen, Bull. Soc. Chim. Belg. 104 (1995) 283.

[27] M. Sanchez, F. Ruette, J. Mol. Struct. Theochem 254 (1992) 335.

[28] K.B. Wiberg, Tetrahedron 24 (1968) 1083.

[29] G. Blyholder, J. Head, F. Ruette, Theor. Chim. Acta 60 (1982) 429.

[30] F. Ruette, A. Sierraalta, A. Hernández, in: F. Ruette (Ed.), Quantum Chemistry Approaches to Chemisorption and Heterogeneous Catalysis, Kluwer, Dordrecht, 1992, p. 320 and references therein.

[31] F. Ruette, F.M. Poveda, A. Sierraalta, M. Sánchez, E.N. Rodríguez-Arias, J. Mol. Catal. 119 (1997) 335.

[32] M. Sánchez, L.S. Rodríguez, G. Larrazabal, L. Galean, N. Bello, F. Ruette, Lect. Ser. Comput. Comp. Sci. 1 (2004) 1219.
[33] M. Sánchez, L.S. Rodríguez, G.Larrazabal, L.Galean, N. Bello, F. Ruette, J. Comp. Appl. Math, submmited for publication.
[34] F.M. Allen, Acta Cryst. B 58 (2002) 380.
[35] P.E.M. Siegbahn, R.H. Crabtree, J. Am. Chem. Soc. 119 (1997) 3103.